



LAWRENCE  
LIVERMORE  
NATIONAL  
LABORATORY

UCRL-CONF-201697

# Simulated $(n,f)$ cross section of isomeric $^{235\text{m}}\text{U}$

*W. Younes, H.C. Britt, and J.A. Becker*

**December 18, 2003**

NEDPEC 2003, Los Alamos, New Mexico  
October 20-24, 2003

This document was prepared as an account of work sponsored by an agency of the United States Government. Neither the United States Government nor the University of California nor any of their employees, makes any warranty, express or implied, or assumes any legal liability or responsibility for the accuracy, completeness, or usefulness of any information, apparatus, product, or process disclosed, or represents that its use would not infringe privately owned rights. Reference herein to any specific commercial product, process, or service by trade name, trademark, manufacturer, or otherwise, does not necessarily constitute or imply its endorsement, recommendation, or favoring by the United States Government or the University of California. The views and opinions of authors expressed herein do not necessarily state or reflect those of the United States Government or the University of California, and shall not be used for advertising or product endorsement purposes.

This work was performed under the auspices of the U.S. Department of Energy by University of California, Lawrence Livermore National Laboratory under Contract W-7405-Eng-48.

# Simulated $(n, f)$ cross section of isomeric $^{235m}\text{U}$

W. Younes,\* H. C. Britt, and J. A. Becker

Lawrence Livermore National Laboratory, Livermore, CA 94551

(Dated: December 18, 2003)

The neutron-induced fission cross section on the  $^{235}\text{U}$ ,  $T_{1/2} \approx 26$  min isomer has been deduced for incident neutron energies in the range  $E_n = 0.1 - 2.5$  MeV, using the surrogate-reaction technique. In this technique,  $^{236}\text{U}$  fission probabilities measured in the  $^{234}\text{U}(t, pf)$  reaction have been converted into  $^{235}\text{U}(n, f)$  and  $^{235m}\text{U}(n, f)$  cross sections, using reaction theory to compensate for the differences in angular-momentum and parity distributions in the fissioning systems, transferred by the  $(t, p)$  and neutron-induced reactions. Based on the comparison between the  $^{235}\text{U}(n, f)$  cross section extracted in this work and independent experimental data, the deduced  $^{235m}\text{U}(n, f)$  cross section is believed to be reliable to 20% below  $E_n \approx 0.5$  MeV and 10% at higher energies. The surrogate-reaction technique, its validation in the case of the  $^{235}\text{U}(n, f)$  cross section, and the deduced  $^{235m}\text{U}(n, f)$  cross section are discussed. Validation of this method allows  $(n, f)$  cross sections for many short-lived nuclei, as well as isomeric nuclei, to be extracted from measured fission probabilities.

## I. INTRODUCTION

The neutron-induced fission cross section on the  $T_{1/2} \approx 26$  min isomer in  $^{235}\text{U}$  can be important in environments where this isomer is exposed to an energetic neutron flux. Because of the relatively short half-life of this isomer, it is extremely difficult to prepare a  $^{235m}\text{U}$  target for a direct laboratory measurement of the  $^{235m}\text{U}(n, f)$  cross section. Measurements at cold- and thermal-neutron energies [1] suggest that the  $^{235m}\text{U}(n, f)$  cross section is significantly larger than the  $(n, f)$  cross section on the  $^{235}\text{U}$  ground state. However, these measurements carry large uncertainties, and no experiments have been performed at higher incident neutron energies.

In this paper, we obtain an experimentally determined  $^{235m}\text{U}(n, f)$  cross section by using a different, more feasible reaction as a surrogate for the  $(n, f)$  reaction. The  $^{234}\text{U}(t, pf)$  reaction populates the same fissioning system,  $^{236}\text{U}$ , as does the  $n + ^{235}\text{U}$  reaction. With the help of reaction modeling, the difference in the angular momentum and parity distributions transferred in the  $(t, p)$  and  $n$ -induced reactions can be accounted for, and the  $(n, f)$  cross section can be deduced from measured  $(t, pf)$  fission probabilities.

The experimental data used in this paper are presented in section II. The formalism of the surrogate-reaction method is briefly discussed in section III. In section IV, the  $(n, f)$  cross section on the  $^{235}\text{U}$  ground state is deduced from  $^{234}\text{U}(t, pf)$  data using the surrogate technique, and compared to an ENDF/B-VI [2] evaluation of independent experimental data, as a validation of the technique. The  $(n, f)$  cross section on the  $^{235}\text{U}$  isomer is then extracted for incident neutron energies  $E_n = 0.1 - 2.5$  MeV, and compared to the  $(n, f)$  cross section on the ground state.

## II. EXPERIMENTAL DETAILS

The data used in this paper consist of fission probabilities in the  $^{234}\text{U}(t, pf)$  reaction, measured as a function of excitation energy in the compound  $^{236}\text{U}$  system by Britt *et al.* [3]. A  $^{234}\text{U}$  target was bombarded with 18-MeV tritons. A small solid-angle telescope, situated at  $140^\circ$  with respect to the beam direction, was used to identify the outgoing proton and measure its energy, with an energy resolution of approximately 120 keV (full width at half maximum). Phosphorus-diffused silicon detectors were used to detect fission fragments.

The  $(t, pf)$  fission probability was measured as the fraction of detected outgoing protons that were accompanied by a fission event, corrected for detector efficiency. The excitation energy of the fissioning nucleus was reconstructed from the measured proton energy and the kinematics of the reaction. A background subtraction was applied to the proton singles data in order to eliminate the effect of contaminants. A  $\pm 10\%$  systematic uncertainty is associated with the data because of the background subtraction. Because of the inherent energy resolution of the proton detector, the cross section deduced from the  $(t, pf)$  has a range of validity limited to  $E_n \gtrsim 100$  keV.

---

\*Electronic address: younes@llnl.gov

### III. MODEL

A sketch of the surrogate method used to convert measured  $(t, pf)$  fission probabilities to estimated  $(n, f)$  cross sections is given in this section. A more detailed description of the formalism can be found in [4].

The basic assumption of the surrogate method is that the  $(t, pf)$  reaction proceeds in two sequential steps: 1) a compound system is formed by a fast direct  $(t, p)$  reaction and 2) after a comparatively long time, the equilibrated nucleus fissions. Thus the formation and subsequent fission processes can be separated, and the only connection between the two steps are the quantum numbers of the system: the excitation energy  $E_x$ , the total angular momentum  $J$  and the parity  $\pi$ . Formally, the separation of the  $(t, pf)$  reaction into two steps is written

$$P_{(t,pf)}(E_x) = \sum_{J^\pi} P_{(t,p)}(J^\pi) \times P_f(E_x, J^\pi), \quad (1)$$

where  $P_{(t,pf)}(E_x)$  is the probability of fission via the  $(t, pf)$  reaction for a given excitation energy  $E_x$  of the compound system,  $P_{(t,p)}(J^\pi)$  is the probability of forming a compound system with spin and parity  $J^\pi$  via the  $(t, p)$  reaction, and  $P_f(E_x, J^\pi)$  is a reaction-independent probability that a compound state with quantum numbers  $E_x$ ,  $J$ , and  $\pi$  will fission. The sum in Eq. (1) extends over all possible spins and parities of the compound system. The range of excitation energies considered in this paper will be fairly small, therefore the excitation-energy dependence of the probability  $P_{(t,p)}$  in Eq. (1) has been ignored. Similarly, the  $(n, f)$  reaction can be decomposed into sequential formation and fission processes. As a result, the  $(n, f)$  cross section is written

$$\sigma_{(n,f)}(E_n) = \sum_{J^\pi} \sigma_{CN}(E_n, J^\pi) \times P_f(E_x, J^\pi), \quad (2)$$

where  $E_n$  is the incident neutron energy, which is related to the excitation energy  $E_x$  by  $E_n = E_x - B_n$ , with  $B_n = 6.545$  MeV, the binding energy of the neutron in the  $n + {}^{235}\text{U}$  system. The compound-nucleus formation cross section is given by  $\sigma_{CN}(E_n, J^\pi)$ .

The essence of the surrogate method consists in recognizing that the probability  $P_f(E_x, J^\pi)$ , in Eqs. (1) and (2), is the same quantity. The probability  $P_{(t,pf)}(E_x)$ , which appears on the left-hand side of Eq. (1) is measured experimentally, and therefore the fission probability  $P_f(E_x, J^\pi)$ , which appears on the right-hand side of Eq. (1) can be constrained. The same constrained probability  $P_f(E_x, J^\pi)$  is then used in Eq. (2) to estimate the  $(n, f)$  cross section. The formation of the fissioning system in Eqs. (1) and (2) must still be modeled, but the underlying theory well-understood. The advantage of the surrogate method is that the fission process, which is less well understood, is constrained by experimental  $(t, pf)$  data. The  $(t, p)$  formation probability,  $P_{(t,p)}$ , in Eq. (1) is modeled by a distorted-wave Born approximation (DWBA), as described in [4]. The compound-nucleus formation cross section,  $\sigma_{CN}$ , in Eq. (2) is calculated using transmission coefficients obtained from an optical model [5]. The fission probability  $P_f(E_x, J^\pi)$  is calculated using the Bohr transition-state model, represented schematically in Fig. 1, grafted onto a modified version of the double-hump fission-barrier model. Starting from a state with given excitation energy, spin, and parity in the first well in Fig. 1, (for sufficiently-low excitation energy) the nucleus can decay by three independent modes, which are allowed to compete statistically:  $\gamma$  decay within the first well, neutron decay into the first well of the residual nucleus, or fission across the inner barrier  $A$ , and then across one of two possible outer barriers  $B$ , or  $B_{II}$ . In the transition-state hypothesis the passage across the barriers, starting from a state with spin and parity  $J^\pi$  in the first well, requires the presence of states with the same spin and parity at nearby energies. Although the level energy is a continuous function of deformation, it only needs to be specified in the first well and on top of the barriers. For these levels, a set of discrete states based on experimental evidence are used and augmented by allowing the coupling between the states. At pairing-gap energies,  $\approx 1.2$  MeV in the first well and  $\approx 1.7$  MeV on top of the barriers, the discrete levels are replaced by continuous level densities, calculated using a microscopic-macroscopic model.

The surrogate technique formalized in Eqs. (1) and (2) improves on earlier attempts [6] to deduce the  ${}^{235}\text{U}(n, f)$  cross section from measured  $(t, pf)$  probabilities in two ways:

1. In the earlier work, spin and parity were not taken into account and the  $(n, f)$  cross section was estimated using the simple formula

$$\sigma_{(n,f)}(E_n) = \sigma_{CN}(E_n) \times P_{(t,pf)}(E_x). \quad (3)$$

Eq. (3) does not correctly incorporate the physics of angular-momentum and parity conservation and, therefore, cannot be expected to be as reliable as Eqs. (1) and (2).

2. Because they account for spin and parity, Eqs. (1) and (2) can be used to estimate the  $(n, f)$  cross section on the isomeric  $^{235m}\text{U}(n, f)$  state at  $E_x \approx 77$  eV, since the ground state ( $J^\pi = 7/2^-$ ) and isomer ( $J^\pi = 1/2^+$ ) differ essentially only by their spins and parities.

#### IV. RESULTS

The  $P_{(t,pf)}(E_x)$  data of Britt *et al.* [3] have been fitted using the model described in section III. The only free parameters in the model are the fission barrier heights,  $E_A$ ,  $E_B$ , and  $E_{B_{II}}$ , corresponding to the inner barrier  $A$  and the outer barriers  $B$  and  $B_{II}$  displayed in Fig. 1. Furthermore, the height of the second outer barrier,  $E_{B_{II}}$  has been fixed in the present calculations to the value  $E_{B_{II}} = 6.40$  MeV, in accordance with independent experimental evidence [7]. The remaining barrier heights,  $E_A$  and  $E_B$  are fitted to the measured  $P_{(t,pf)}(E_x)$  data below the neutron binding energy. The best fit is shown in the top panel of Fig. 2. The quality of the fit deteriorates for  $E_x \gtrsim B_n$ . This deterioration is caused by a mismatch between the number of discrete and continuous levels at the pairing gap, where the continuous level-density formalism is allowed to take over from discrete states. Although the absolute fission probabilities  $P_f(E_x, J^\pi)$  suffer from this mismatch, it is expected that their values relative to one another are still reliable. In order to compensate for the discrepancy in the fit, the  $(n, f)$  cross section estimated using Eq. (2) is renormalized to the experimental  $(t, pf)$  data after the fit,

$$\sigma_{(n,f)}(E_n) \rightarrow \sigma_{(n,f)}(E_n) \times \frac{P_{(t,pf)}^{(\text{expt})}(E_x)}{P_{(t,pf)}^{(\text{calc})}(E_x)}, \quad (4)$$

where the superscripts “(expt)” and “(calc)” have been used to differentiate the  $P_{(t,pf)}$  probability measured experimentally from the quantity calculated in Eq. (1), respectively. The estimated  $^{235}\text{U}(n, f)$  cross section is shown in the bottom panel of Fig. (2) and compared to the previous estimate by Cramer *et al.* [6], and the ENDF/B-VI evaluation, which is believed to be accurate at the 2% level or less, for all neutron energies. The simulated cross section generally agrees with the ENDF/B-VI evaluation within  $\pm 10\%$  uncertainties, except for an approximate 20% overshoot in the region of 0.2 to 0.5 MeV. The overall agreement is remarkably good. This comparison involves no adjustable parameters so that the agreement implies that the surrogate procedure, the absolute fission probability measurements, and the calculated neutron compound cross sections are collectively accurate to approximately 10%. (Although the possibility of larger errors, which cancel in the product, cannot be ruled out.) The current calculation also represents a significant improvement over the earlier Cramer *et al.* [6] estimate. The improvement is likely due to a combination of the proper inclusion of spin and parity in the calculation, and a more reliable evaluation of the neutron transmission coefficients [5].

The result shown in the bottom panel of Fig. (2) validates the surrogate method in the case of the  $(n, f)$  cross section on the  $^{235}\text{U}$  ground state. The extension of the surrogate method to the calculation of the  $(n, f)$  cross section on the  $^{235}\text{U}$  isomer is relatively straightforward. The fission probability  $P_f(E_x, J^\pi)$  determined for the ground-state cross section is used directly in Eq. (2) to estimate the  $^{235m}\text{U}(n, f)$  cross section. The compound nucleus cross section  $\sigma_{CN}(E_n, J^\pi)$  is recalculated for a spin-1/2  $^{235m}\text{U}$  target, instead of the spin-7/2 value of the  $^{235}\text{U}$  ground state. The renormalization procedure in Eq. (4) is applied. The resulting  $^{235m}\text{U}(n, f)$  cross section is plotted in Fig. 3a). The isomer-to-ground-state ratio of  $(n, f)$  cross sections is shown in Fig. 3b). Based on the  $^{235}\text{U}(n, f)$  result, the estimated  $^{235m}\text{U}(n, f)$  cross section is expected to be reliable to within 20% for  $E_n \lesssim 0.5$  MeV, and 10% for  $E_n \gtrsim 0.5$  MeV.

The important feature of the isomer-to-ground-state ratio plotted in Fig. 3b) is that fission from the isomeric level is inhibited relative to fission from the ground state. This effect can be understood in terms of the transition states on top of the barrier. It is known from experimental evidence that  $0^-$  and  $1^+$  states are relatively rare below the pairing gap. On the other hand, the  $0^-$  and  $1^+$  states provide paths for the nucleus to transit across the barriers in low-energy neutron-induced fission of the isomeric  $J^\pi = 1/2^+$  state. The paucity of these special states weakens the  $^{235m}\text{U}(n, f)$ , while no such effect is present in the calculation of the  $^{235}\text{U}(n, f)$  cross section. The effect can also be seen in the fission probabilities  $P_f(E_x, J^\pi)$ , plotted in Fig. 4. The probabilities for the  $J^\pi = 0^-$  and  $1^+$  states are the weakest in Fig. 4. All the  $P_f(E_x, J^\pi)$  curves converge to the same value for  $E_x \gtrsim 8$  MeV, because the angular-momentum dependence of the fission, neutron-emission and  $\gamma$ -decay widths become purely statistical and therefore identical at higher excitation energies, and that dependence cancels out in the calculation of the probability as a ratio of the competing processes.

## V. CONCLUSION

The  $(n, f)$  cross section on the  $^{235}\text{U}$  isomeric state at  $E_x = 77$  eV has been deduced from measured  $^{234}\text{U}(t, pf)$  fission probabilities in the equivalent energy range  $E_n = 0.1 - 2.5$  MeV, using the surrogate-reaction technique. The technique has been validated by extracting the  $(n, f)$  cross section on the  $^{235}\text{U}$  ground state and comparing it to a reliable evaluation from the ENDF/B-VI database. Based on this validation, the estimated  $^{235m}\text{U}(n, f)$  cross section is expected to be accurate to 20% below  $E_n = 0.5$  MeV, and 10% at higher energies. The  $^{235m}\text{U}(n, f)$  cross section is found to be consistently weaker than the  $(n, f)$  cross section on the  $^{235}\text{U}$  ground state in the  $E_n = 0.1 - 2.5$  MeV range, by as much as  $\approx 70\%$  near  $E_n = 100$  keV, and becoming equal to the ground-state cross section near  $E_n = 2.5$  MeV. This effect is understood in terms of a paucity of  $0^-$  and  $1^+$  transition states near the fission barriers, inhibiting the fission process for low-spin neutron targets, such as the  $1/2^+$  isomeric state in  $^{235}\text{U}$ . In general then, it will be profitable to revisit measured fission probabilities, and analyze them with a proper accounting of spin and parity. In addition, fission probabilities of isomer states can also be predicted. Using the surrogate-reaction technique,  $(n, f)$  cross sections for targets of  $^{231,233}\text{Th}$ ,  $^{234,236,237,239}\text{U}$ , and  $^{240,241,243}\text{Pu}$  have been estimated [8]. Further  $(n, f)$  cross sections for targets of  $^{236,236m,237,238}\text{Np}$ ,  $^{237,237m}\text{Pu}$ ,  $^{240,241,242,242m,243,244,244m}\text{Am}$  are currently being extracted using the same method [9].

## VI. ACKNOWLEDGMENTS

This work was performed under the auspices of the U.S. Department of Energy by the University of California under contract No. W-7405-Eng-48.

- 
- [1] A. D'Eer, C. Wagemans, M. Nève de Mévergnies, F. Gönnenwein, P. Geltenbort, M. S. Moore, and J. Pauwels, Phys. Rev. C **38**, 1270 (1988).
  - [2] L. W. Weston, P. G. Young, W. P. Poenitz, and C. R. Lubitz, ENDF/B-VI evaluation, MAT # 9228, Revision 5, October 1997; data retrieved from the ENDF database.
  - [3] H. C. Britt, F. A. Rickey, and W. S. Hall, Phys. Rev. **175**, 1525 (1968).
  - [4] W. Younes and H. C. Britt, Phys. Rev. C **67**, 024610 (2003).
  - [5] F. S. Dietrich (2001), private communication.
  - [6] J. D. Cramer and H. C. Britt, Nucl. Sci. Eng. **41**, 177 (1970).
  - [7] A. Gavron, H. C. Britt, P. D. Goldstone, J. B. Wilhelmy, and S. E. Larsson, Phys. Rev. Lett. **38**, 1457 (1977).
  - [8] W. Younes and H. C. Britt, Phys. Rev. C **68**, 034610 (2003).
  - [9] W. Younes, H. C. Britt, and J. A. Becker, Tech. Rep., LLNL (2003), manuscript in preparation.

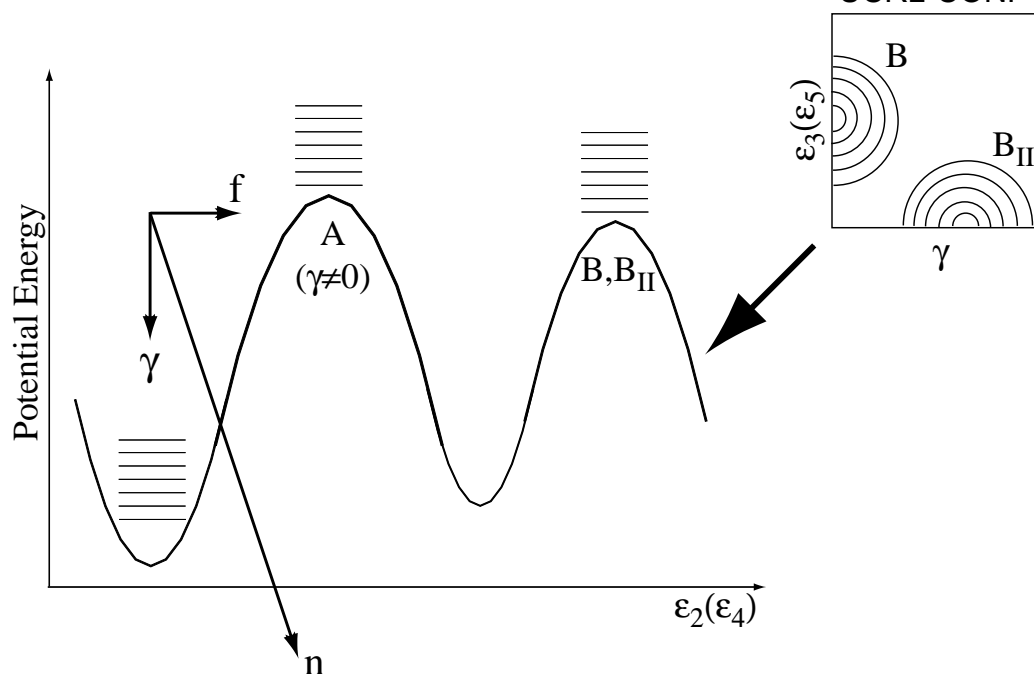


FIG. 1: Schematic representation of the statistical fission model used. The inset shows the difference between barriers  $B$  and  $B_{II}$  encountered along parallel fission paths: barrier  $B$  has a static octupole deformation, whereas barrier  $B_{II}$  is triaxial.

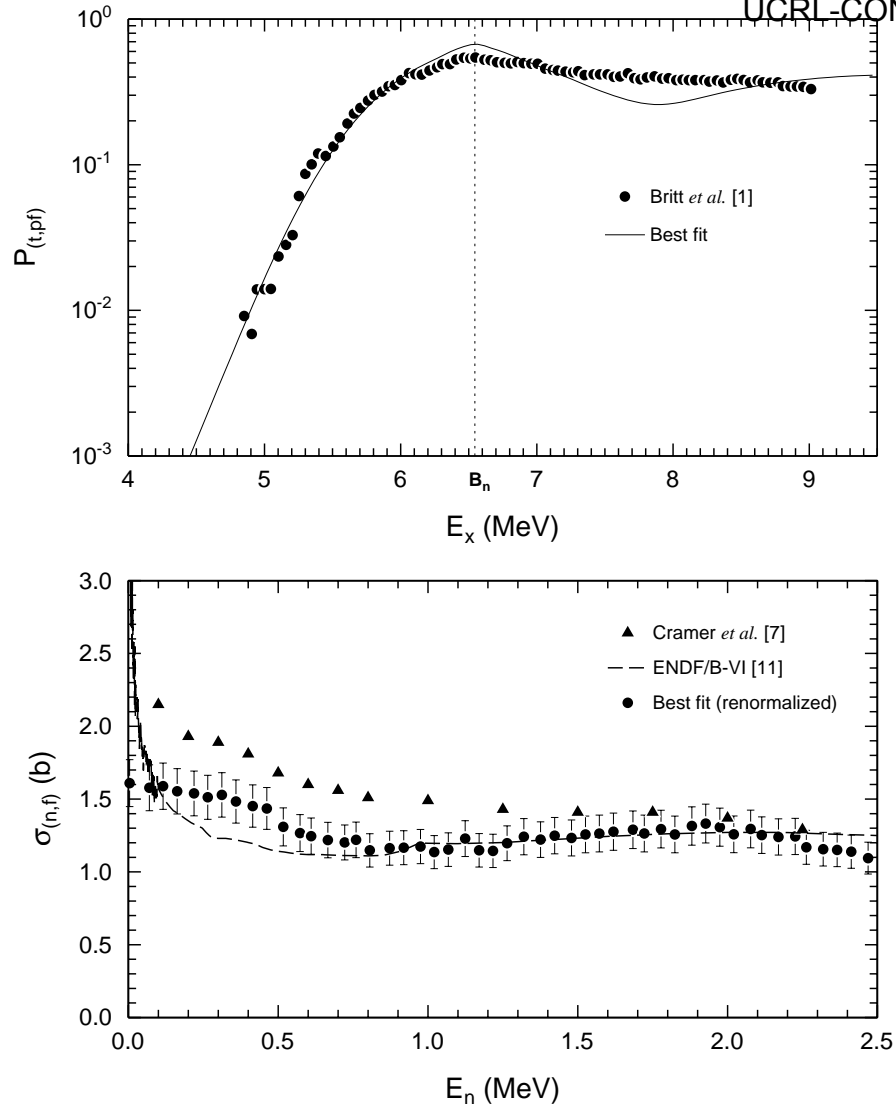


FIG. 2: Best fit to the  $P_{(t,pf)}$  data (top panel), and estimated  $(n,f)$  cross section compared to the original result of Cramer *et al.* [6] and the evaluated ENDF/B-VI values (bottom panel). The dotted line in the top panel indicates the neutron-binding energy value. The error bars on the estimated  $\sigma_{(n,f)}$  values correspond to a 10% systematic uncertainty in the  $P_{(t,pf)}$  data. The Cramer *et al.* cross section carries the same 10% uncertainty associated with the  $P_{(t,pf)}$  data (error bars not shown).



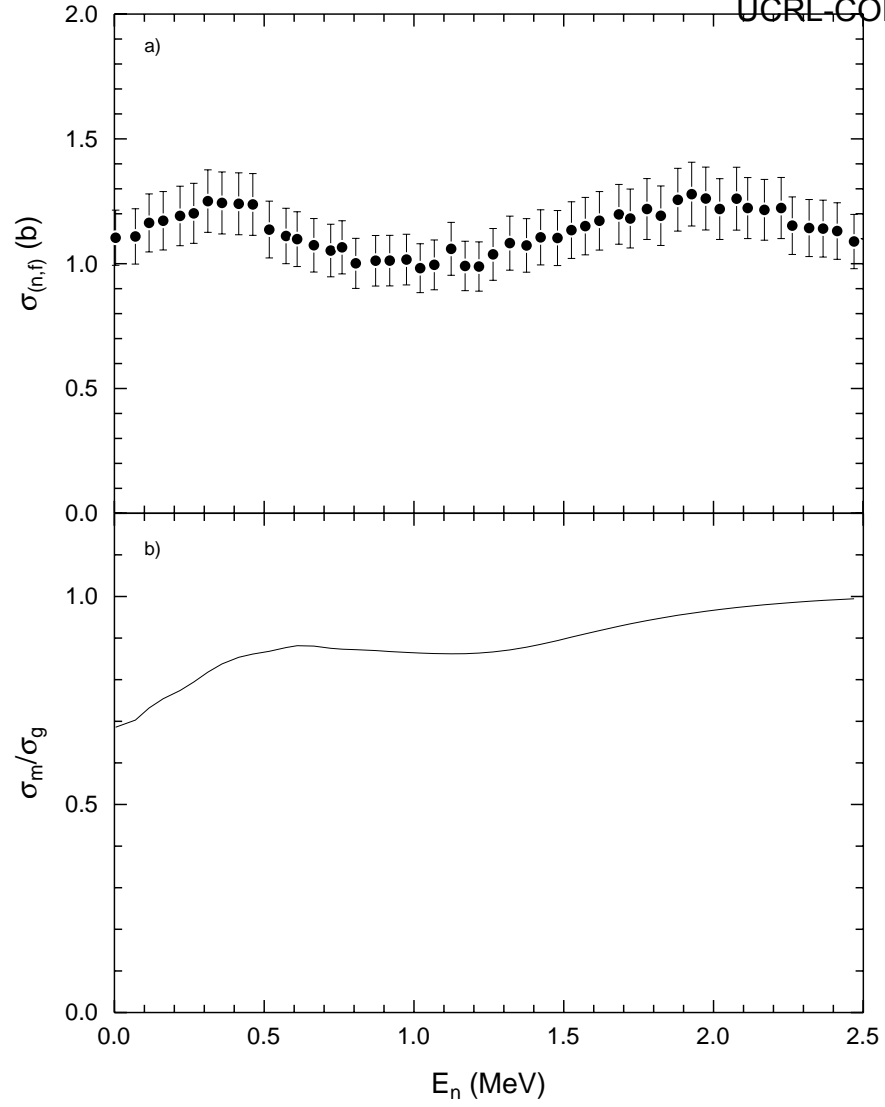


FIG. 3: Best-fit estimates of a) the  $^{235}\text{U}^m(n, f)$  cross section, and b) the isomer-to-ground-state  $(n, f)$  cross section ratio. The error bars on  $\sigma_{(n,f)}$  reflect a 10% systematic uncertainty in the  $P_{(t,pf)}$  data.

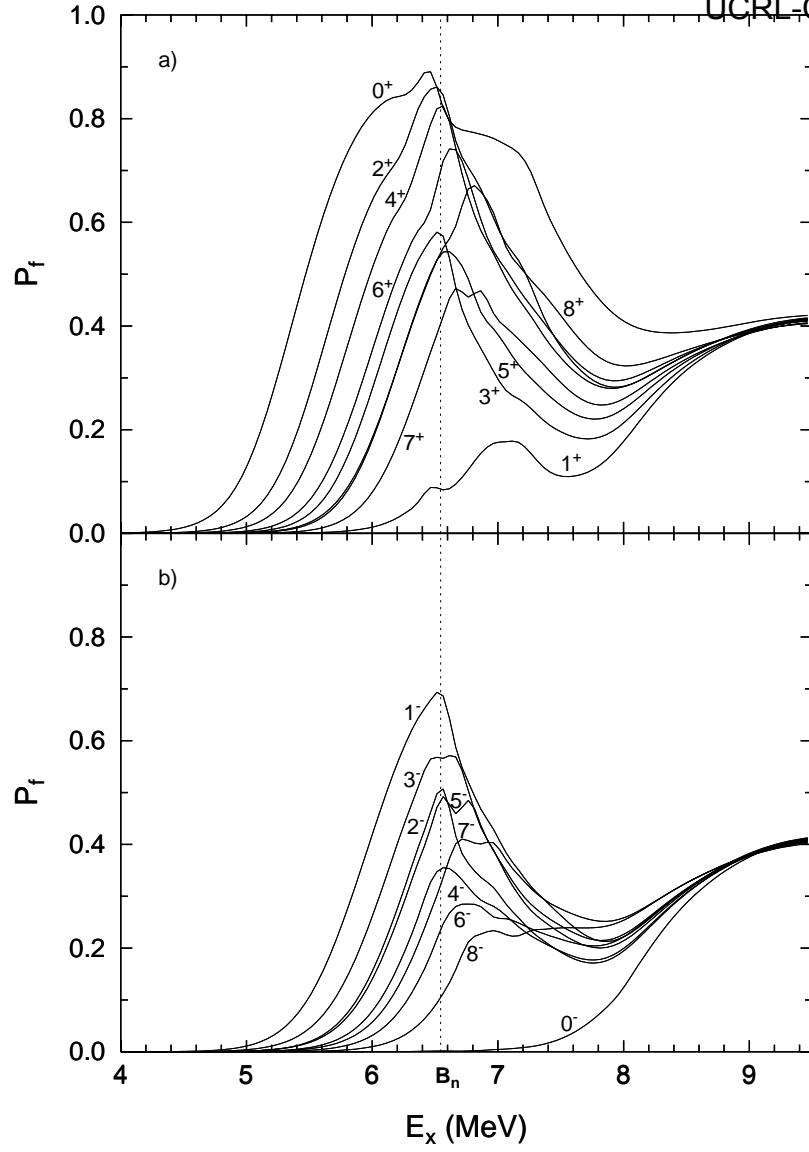


FIG. 4: Best-fit values of the individual fission probabilities  $P_f(E_x, J^\pi)$ , as a function of excitation energy  $E_x$  of the compound nucleus. The positive-parity probabilities are plotted in panel a), while the negative-parity ones are shown in panel b). The dotted vertical line indicates the neutron-binding energy value.